 ©2018 Kvantovaya Elektronika and Turpion Ltd

https://doi.org/10.1070/QEL16843

Enhancement of local electromagnetic fields by periodic optical resonators

A.K. Sarychev, A.V. Ivanov, K.N. Afanasyev, I.V. Bykov, I.A. Boginskaya, I.N. Kurochkin, A.N. Lagarkov, A.M. Merzlikin, V.V. Mikheev, D.V. Negrov, I.A. Ryzhikov, M.V. Sedova

Abstract. **The periodically profiled metasurfaces of silicon and of the same surfaces coated with a thin layer of silver are experimentally investigated to improve the signal-to-noise ratio in the observation of Raman light scattering from molecular compounds. The noise in this case is the unavoidable background molecular luminescence. Our experimental and computer simulation data demonstrate an anomalous optical response due to the excitation of metal-dielectric surface resonances. An enhanced Raman scattering signal is observed from 5,5′-dithiobis(2-nitrobenzoic) acid (DTNB) organic molecules deposited on the metasurface. The proposed metasurface provides a significant enhancement of the RS signal in comparison with the luminescence signal and is an efficient substrate for realising giant Raman scattering of light.**

Keywords: *metasurface, plasmon resonance, dielectric resonators, silicon, nanostructures, giant Raman scattering of light.*

1. Introduction

Recent years have seen a significant growth of interest in high-Q low-loss optical resonators in connection with their wide use in basic and applied research. The excitation of surface plasmons in metallic nanoparticles is frequently used for enhancing local electric fields [1]. However, the optical response of metals is damped by the high ohmic loss arising from interband and intraband transitions as well as by the surface scattering of electrons. A common drawback of all nanostructured metals employed in the investigation of surface-enhanced Raman scattering (SERS) of light is the chemical instability and degradation in the air, which is responsible for uncontrollable changes of their surfaces. Gold nanostructures are most stable; however, gold exhibits a high interband loss in the blue part of the visible range ($\lambda < 600$ nm) [2].

A.K. Sarychev, A.V. Ivanov, K.N. Afanasyev, I.V. Bykov, I.A. Boginskaya, A.N. Lagarkov, A.M. Merzlikin, I.A. Ryzhikov, M.V. Sedova
Institute of Theoretical and Applied Electrodynamics, Russian Academy of Sciences, ul. Izhorskaya 13, 125412 Moscow, Russia; e-mail: sarychev_andrey@yahoo.com;
I.N. Kurochkin N.M. Emanuel Institute for Biochemical Physics, Russian Academy of Sciences, ul. Kosygina 4, 119334 Moscow, Russia; Department of Chemistry, M.V. Lomonosov Moscow State University, Vorob'evy gory, 119991 Moscow, Russia;
V.V. Mikheev, D.V. Negrov Moscow Institute of Physics and Technology (State University), Institutskii per. 9, 141701 Dolgoprudnyi, Moscow region, Russia

Received 9 October 2018; revision received 18 October 2018
Kvantovaya Elektronika **48** (12) 1147–1152 (2018)
Translated by E.N. Ragozin

Dielectric resonators are an obvious alternative to metallic nanoparticles. Electromagnetic resonances may be excited in any low-loss dielectric sample. Whispering gallery modes may be highest in Q-factor ($Q = 10^7$–10^9 [3–8]) among all electromagnetic modes. Optical resonators in which whispering gallery modes are realised can be made of silicon, as well as of III–V group semiconductors, and may have the shape of a disk, sphere, cylinder, or a torus.

The general analytic solution for a surface plasmon excited in a thin metallic film of modulated thickness was first obtained by Dyknhe et al. [9], who showed that the film sees an enhancement of optical effects, including the emergence of optical bistability. Plasmon modes excited in metal–dielectric multilayer structures were investigated in Refs [10–23]. The authors of Ref. [16] consider a ring of metallic nanoparticles interacting with each other as well as with an adjacent dielectric microresonator. Plasmon resonance in the ring gives rise to a significant enhancement of the electromagnetic field near the dielectric microresonator surface away from the ring. It is noteworthy that the field is less enhanced in the case of separated metallic nanoparticles and dielectric microresonators [15]. The propagation of light in dielectric metamaterials is discussed in review Ref. [22]. The enhancement of electric field and the SERS effect in periodic metafilms based on dielectric microridges were investigated in the microwave and optical regions in Refs [13, 21, 24–28]. Dielectric resonances in cerium-based random faceted metafilms were considered in Ref. [29]. The experimental observation of SERS enhancement in silver nanoparticles on the surface of porous silicon is discussed in Ref. [30].

In the present work we investigate the interaction of light with the dielectric metasurface formed of periodic silicon ridges with a thin surface silver layer. The metasurface may be the host of metal-dielectric resonances in the visible and near-infrared spectral regions. The SERS effect is demonstrated on such silicon metasurface with 5,5′-dithiobis (2-nitrobenzoic) acid (DTNB) molecules deposited on it, which fulfil the function of an indicator of the local enhancement of optical electromagnetic field.

2. Sample preparation

In the investigation of RS, the observation of the useful RS signal is hindered by the presence of background luminescence. Use is therefore made of various means and techniques to improve the RS-to-luminescence intensity ratio (the signal-to-noise ratio). We propose a new approach to the solution of this problem and, for this purpose, investigate the silicon metasurface made in the form of microridges. The main

advantage of using silicon as the base material is that luminescence is practically nonexistent in silicon in the interaction with optical radiation. Furthermore, for the visible part of the spectrum the refractive index $n + ik$ of silicon is high and the loss is low: for instance, for $\lambda = 700$ nm $n \approx 3.8$ and $k \approx 0.01$ (Fig. 1).

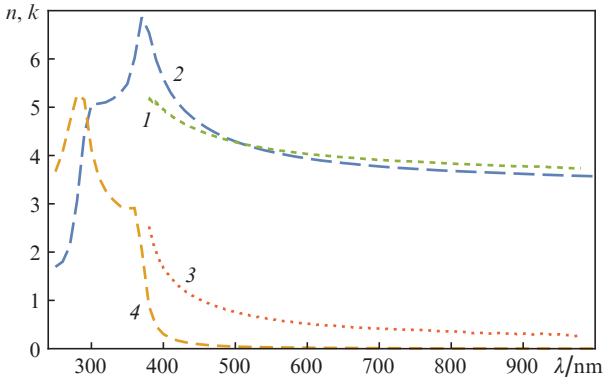

Figure 1. Experimentally measured (*1*,*2*) real n and (*3*,*4*) imaginary k parts of the refractive index of silicon; (*1*,*3*) present work, (*2*,*3*) data borrowed from Ref. [31].

The optical loss in silicon in the visible part of the spectrum increases with decreasing wavelength. Since the SERS signal enhancement coefficient G is approximately proportional to the fourth power of the local electric field, $G \cong |E(r)/E_0|^4 \sim Q^4$ (see Ref. [1], Section 3.6), to enhance the RS signal by three orders of magnitude it would be sufficient to obtain a Q-factor $Q > 5$. Silicon ridges (Fig. 2) may be considered as 'dielectric' resonators. The Q-factor of a silicon resonator is limited by ohmic loss for any configuration, since the Q-factor is estimated as $Q \approx n/k > 5$. Silicon-based metasurfaces may therefore be employed as substrates for increasing the SERS intensity (SERS substrates) in the range of wavelengths longer than ~550 nm.

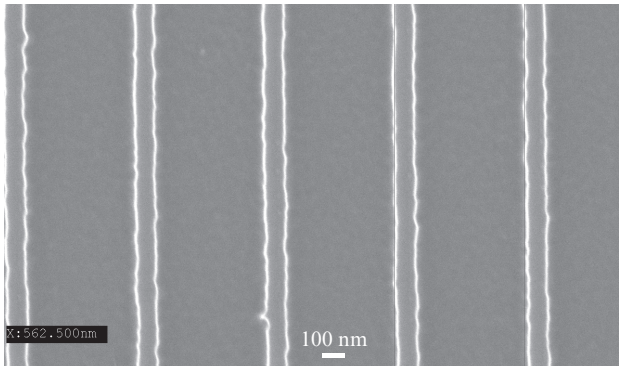

Figure 2. SEM image of the silicon metasurface with the following parameters: period of 560 nm, ridge height of 70 nm, and width of 120 nm.

We consider a metasurface in the form of Si (100) microridges (Fig. 2). The structure was formed on the Si (100) substrate using high-resolution electron-beam lithography (Crestec CABL 9000C machine) and subsequent ion etching of silicon (CORIAL 200I etch tool). To achieve the required size of ridges and valleys, the etching was performed through an APR 6200.04 electron resist in an SF_6/Ar gas mixture with a high DC bias voltage. A high bias voltage in a dry etching process results in a high resist etching rate, and the hollow depth is therefore limited by resist thickness (80 nm). The resist layer was preliminarily exposed to an accelerating voltage of 50 kV and an irradiation dose of 160 μQ cm^{-2}, after which was processed with AR 600-546 developer. After resist removal, in one of the series the surface of silicon substrates was coated with a thin silver layer of thickness ~20 nm by electron-beam evaporation. The metasurface morphology and its geometrical parameters are shown in Fig. 2.

3. Reflection from the metasurface

The spectral dependence of light reflection for the metasurfaces with and without the deposited silver layer were measured in a range of incidence angles α from 20° to 70° for different light polarisation directions. Four such directions may be singled out. We introduce vector $\boldsymbol{q}$, which is the projection of the light wave vector $\boldsymbol{k}$ on the plane of the metasurface. The polarisation direction whereby the q vector is perpendicular to the ridge direction and the electric field $\boldsymbol{E}$ is in the incidence plane is denoted as $p_\perp$ and the light reflection coefficient is denoted as $R_{p_\perp}$ in this case. Reflection coefficient $R_{p_\parallel}$ corresponds to the case when $\boldsymbol{q}$ and $\boldsymbol{E}$ are parallel to the ridge direction. $R_{s_\parallel}$ corresponds to the case when $\boldsymbol{q}$ is parallel and $\boldsymbol{E}$ is perpendicular to the ridge direction. $R_{s_\perp}$ corresponds to the case when $\boldsymbol{q}$ is perpendicular and $\boldsymbol{E}$ is parallel to the ridge direction. The results of experiments and calculations for the four incident light polarisations show minima in the dependences, which shift as the incidence angle is changed (Figs 3–5).

Figure 3 depicts the spectral dependences of light reflection coefficients for the structure without a surface silver layer. Figure 4 shows similar dependences in the presence of a 20-nm thick silver layer. Figure 5 shows the data of experiments and numerical calculation for the structure with the surface silver layer. The numerical calculations were carried out by finite element method in the COMSOL.

The spectral positions of the main resonances approximately coincide with the wavelength corresponding to the appearance of the first diffraction order and are approximately described by the equation $\lambda = L(1 + \sin\alpha)$, where L is the structure period. It may be assumed that the observed resonances are similar to Wood's resonances and are associated with the excitation of surface waves in the metasurface in the diffraction of the incident wave from the periodic grating. The excitation of plasmon modes and Wood's anomalies in metallic and metal-dielectric periodic gratings was discussed in Refs [23, 32–34]. The optical loss in silver, like in silicon, is low for $\lambda > 500$ nm, and the fall of reflection coefficients below 20% demonstrated in Fig. 4a is due to electric field enhancement in the metasurface (Fig. 6). Consider the reflection coefficient for a small angle of incidence ($\alpha = 20°$) (Fig. 5a). The well pronounced minima near the wavelengths $\lambda = 765$ and 920 nm demonstrate to different types of resonances shown in Fig. 6. The angular position of the observed reflectivity minimum at $\lambda = 765$ nm is defined by the grating period. The first resonance (Fig. 6a) is excited due to diffraction and is concentrated primarily in the domain between the ridges, while the second resonance is generated due to the excitation of a standing wave in metal-dielectric ridges. It is noteworthy that the silver deposition procedure is attended with the deposition of silver particles on the side ridge faces

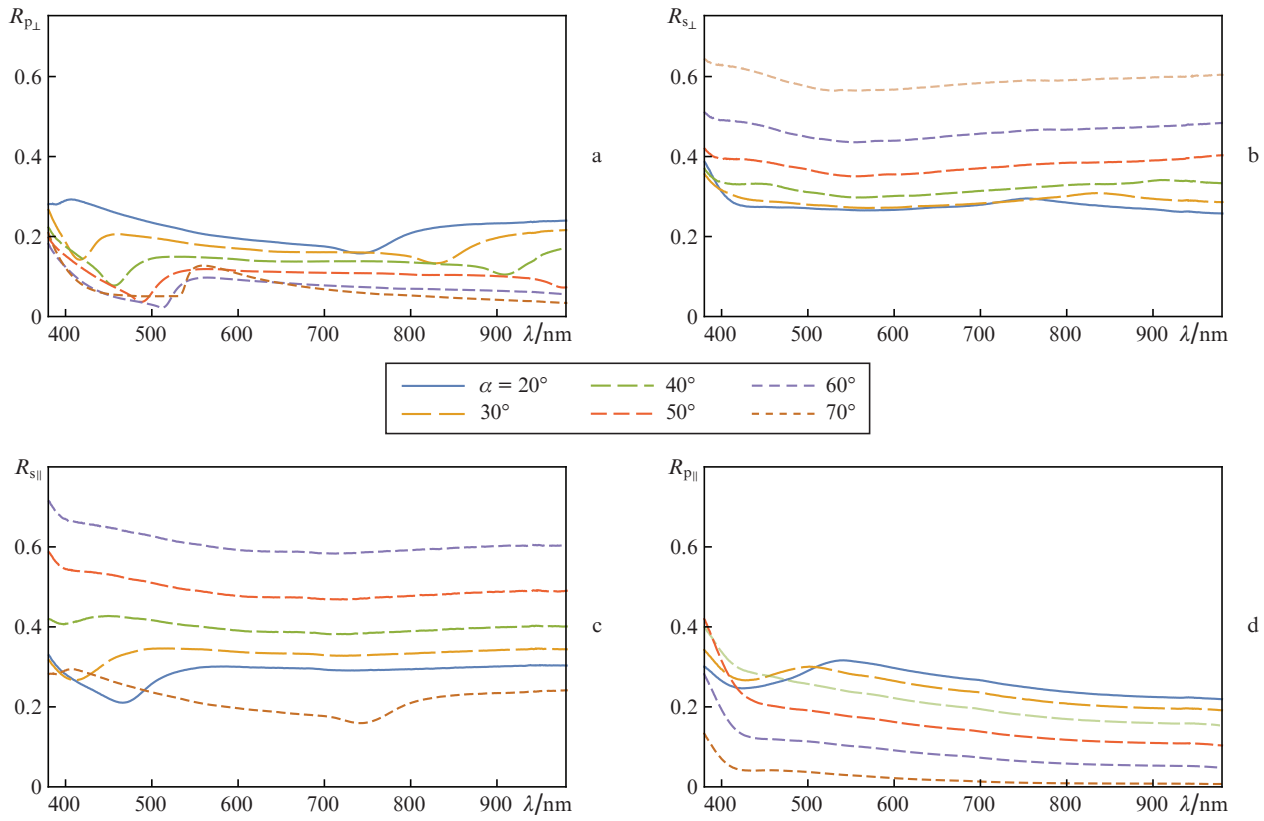

Figure 3. Spectral dependences of the reflection coefficient from the metasurface (Fig. 2) without a silver coating measured for different angles of incidence and polarisations of light.

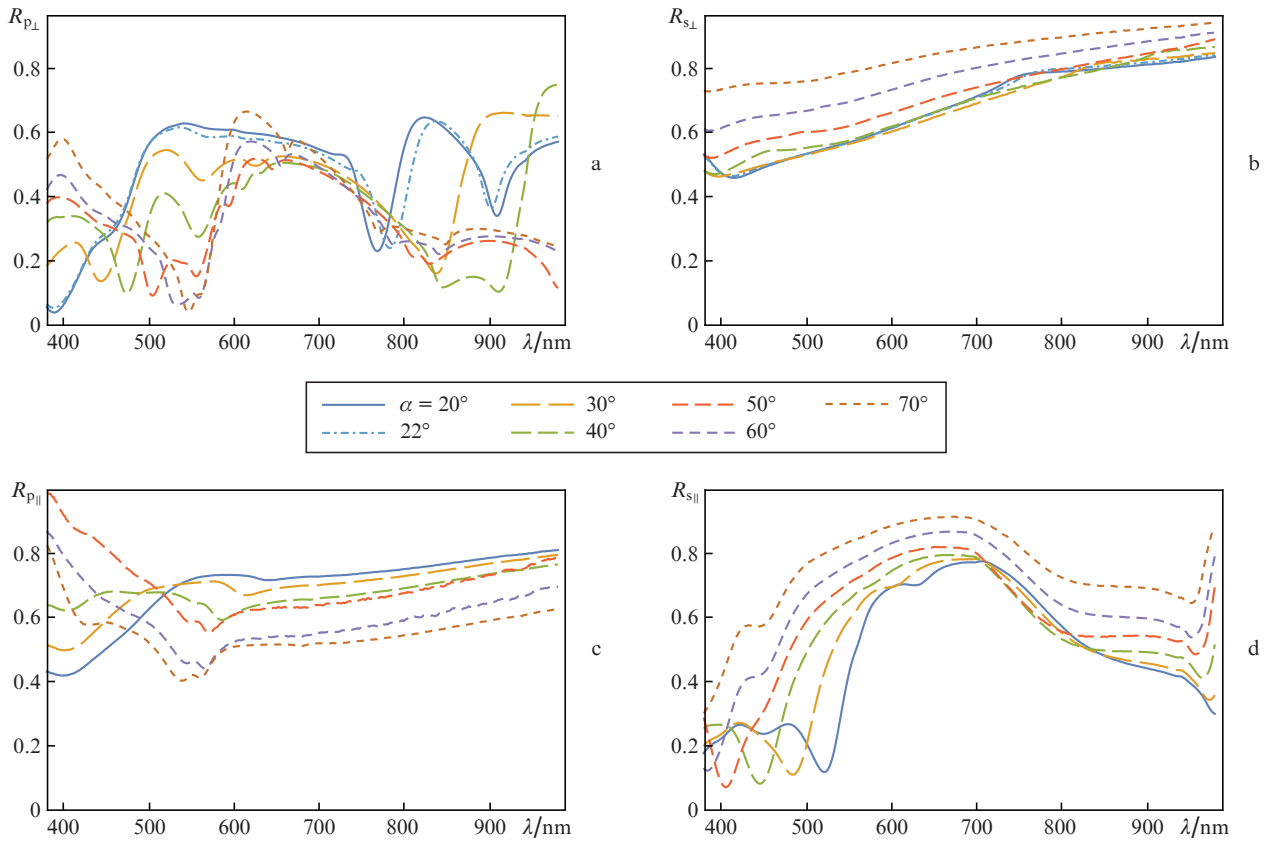

Figure 4. Spectral dependences of the reflection coefficient from the metasurface (Fig. 2) coated with a 20-nm thick silver layer measured for different angles of incidence and polarisations of light.

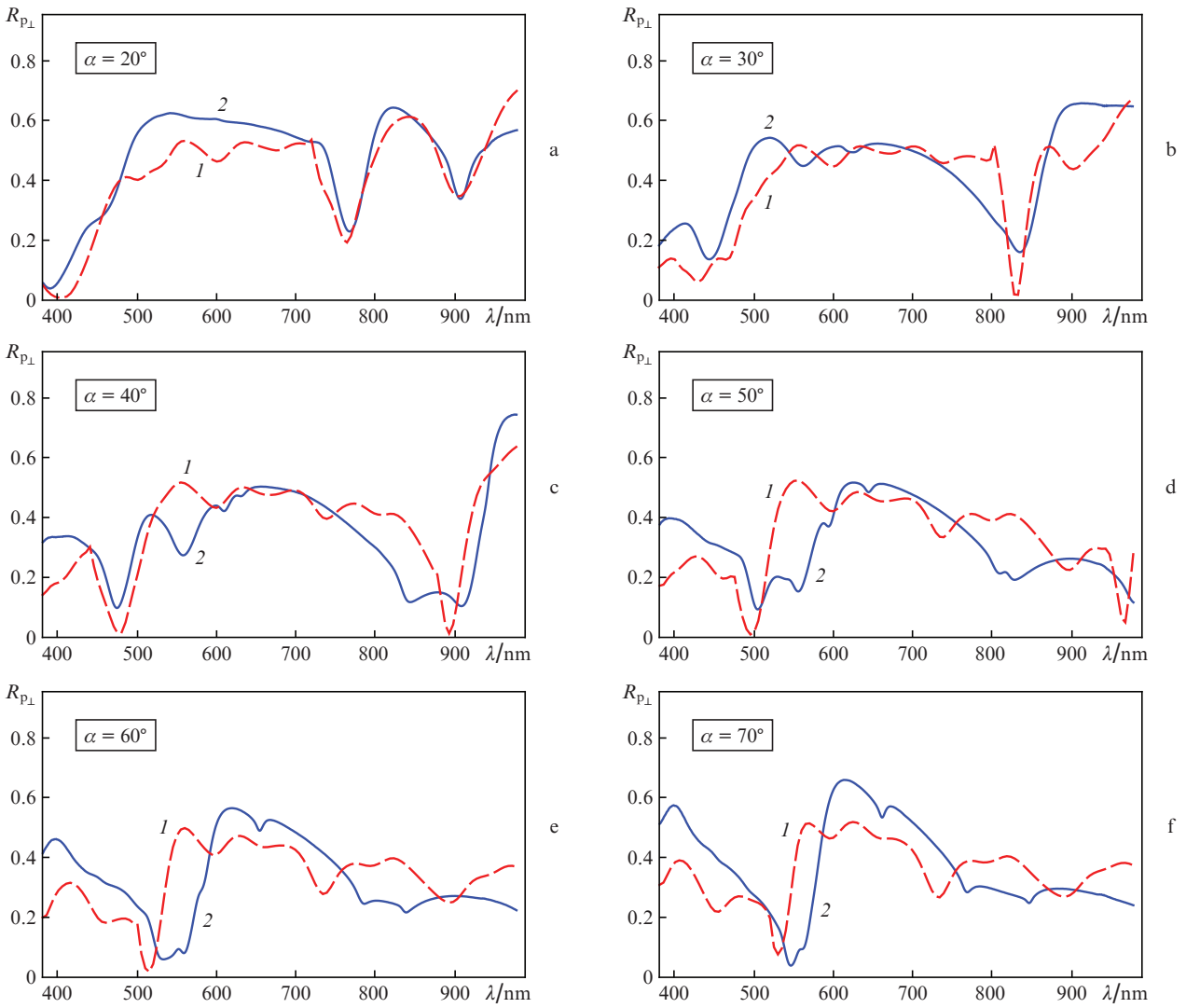

Figure 5. Results of (*1*) computer simulations and (*2*) experimental measurement of the spectral dependences of the reflection coefficient from the silver-coated metasurface. The experiments and simulations were carried out for the following metasurface parameters: 536-nm structure period, 70-nm ridge height, 120-nm ridge width, 25-nm thickness of the silver surface layer, and ~10 nm thick silver layer on the side ridge faces.

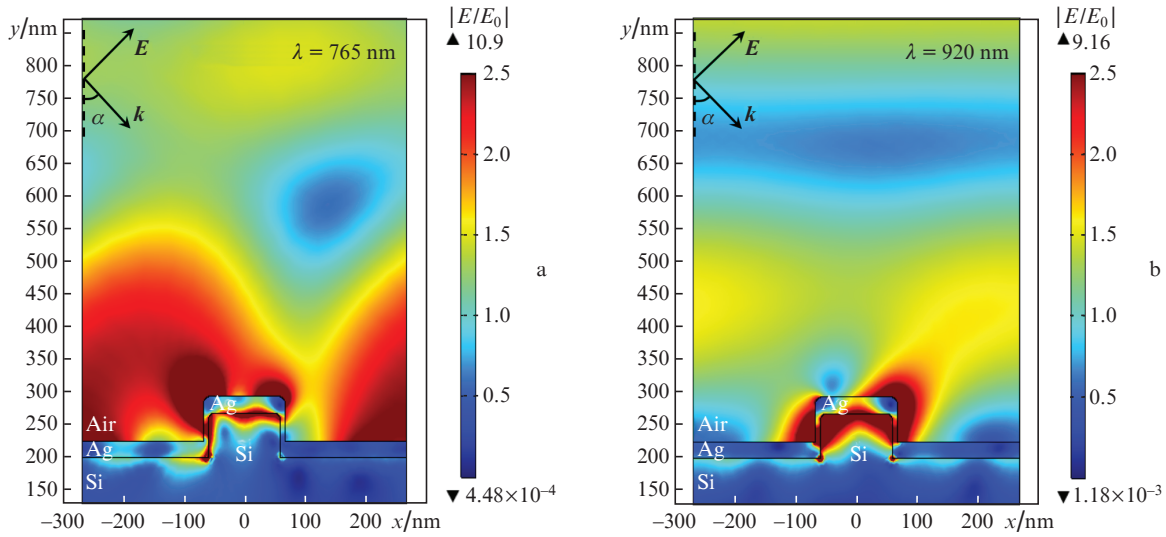

Figure 6. (Colour online) Distributions of the electric field intensity E at the resonance wavelengths (Fig. 5) in the cross section of a unit metasurface cell in the reflection of $p_\perp$-polarised light incident at an angle of 20°; E_0 is the field intensity of the incident light wave.

and not only on the top of the structures domain. Our results suggest: by varying the structure period and the angle of light incidence on the structure it is possible to vary the position of metasurface domains in which the electromagnetic resonances are excited.

4. Signal of Raman light scattering

In the course of experiments we obtained an enhancement of the RS signal by DTNB molecules distributed over the metasurface. DTNB molecules have a well-known RS spectrum and serve as indicators of SERS. An alcohol solution of DTNB with a density of 4 g L^{-1} was prepared for the experiments. DTNB was deposited on the metasurface through a silicone mask made in the form of identical 1-mm deep openings 1.2 mm in diameter. This analyte deposition procedure is caused by the necessity to uniformly distribute DTNB over the metasurface.

The RS spectra excited by $\lambda = 785$ nm laser radiation were recorded with a WiTec spectrometer. Use was made of an objective with a 50$^{\times}$ magnification and a resolution of 500 nm. We investigated the RS spectra of the molecules deposited on the structured sample regions consisting of periodic ridges. Measurements were made of the signals from the silicon metasurface and from the metasurface coated with a thin (20 nm) silver film. The resultant data were compared with the RS signal from the DTNB molecules deposited on the unstructured sample area. Use was made of exciting laser radiation with two polarisation types: with electric field intensity vectors directed along and across the ridges. The duration of every measurement was equal to 10 s and the laser power was equal to ~2 mW. The RS signal was recorded for a Stokes shift frequency of 1338 cm^{-1}. The RS line with this frequency shift relative to the incident light frequency is the strongest line in the RS spectrum of DTNB molecules. The experimental RS signal was averaged over several metasurface regions (Fig. 7). The resultant preliminary data are indicative of a significantly higher intensity of the RS signal from the DTNB molecules in the case of the silver-free ridge-shaped metasurface (p||G, p⊥G in the hystogram) in comparison with the signal recorded in the flat film domain (Si in the hystogram). Furthermore, the RS signal depends on the direction of light polarisation relative to the ridge direction. It is pertinent to note that the main contribution to the increase in SERS intensity is made by the electromagnetic enhancement factor. The 'chemical' contribution to enhancement due to the formation of a chemical bond between the molecules and the substrate depends heavily on the electron structure of the surface as well as of the substrate [35–37]. The 'TNB--metal' chemical bond formation results from the bond breakage of disulfide bridges in DTNB molecules. However, we recorded an RS signal enhancement also for a sample without the silver coating, which may be considered as a demonstration of a purely electromagnetic enhancement of the RS signal. We note that RS signal measurement data obtained for silver-coated samples are ambiguous (the labels Ag20, Ag20(p⊥G), and Ag20(p||G) in the hystogram in Fig. 7). First, there was a significant inaccuracy of the measured data and, second, the problem of nonuniform surface adsorption of the analyte remained unsolved.

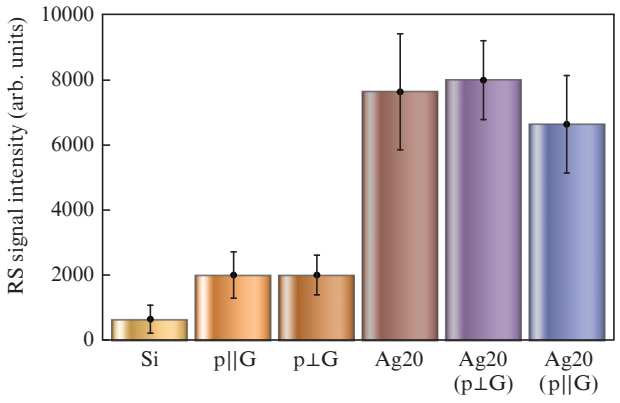

Figure 7. Hystogram of RS signal intensities from various surfaces for the main DTNB Stokes frequency 1338 cm^{-1}; Si is the smooth silicon film surface without a silver surface layer; p||G and p⊥G are structured sample regions without a silver surface layer (metasurface), the electric fields are directed along and across the ridges, respectively; Ag20 is the domain of smooth silicon film with a 20-nm thick silver surface layer; Ag20(p⊥G) and Ag20(p||G) are structured sample domains with the silver surface layer (metasurface), the electric fields are directed across and along the ridges, respectively.

5. Conclusions

We have studied the optical properties of an all-dielectric silicon metasurface as well as of a metal-dielectric metasurface with a thin silver layer on the silicon surface. The results of experiments and computer simulations show the excitation of metal-dielectric resonances, which manifests itself in the dips in the reflection spectra of the samples. The excitation of resonances corresponds to the disappearance of the first diffraction order and is defined by the grating spacing and the angle of light incidence. The resonances excited in the metal-dielectric system correlate with Wood's anomalies arising from the excitation of surface waves on the metasurface due to incident light diffraction by the periodic grating. The resonances may be tuned to the specified wavelengths by varying the shape, geometrical parameters and arrangement of the periodic elements on the metasurface as well as by varying the angle of light incidence on it. Achieved in the metasurface is a high RS-to-luminescence signal ratio, which permits considering it as an efficient SERS substrate. The RS signal from the DTNB molecules immobilised on the metasurface is significantly enhanced in comparison with the signal on a smooth film due to electromagnetic enhancement of the local optical field.

Acknowledgements. This work was supported by the Russian Foundation for Basic Research (Grant Nos 17-08-01448 and 18-58-00048), the Presidium of the Russian Academy of Sciences (Development of Ultrahigh-Sensitivity Techniques for the Identification of Biological Objects With the Aid of Optical Metamaterials and Basic Foundations of Dual-Use Technologies in the Interests of National Security Programmes Nos 40 and 56), as well as by the Ministry of Education and Science of the Russian Federation with the use of equipment of MIPT's Centre for the Shared Use of Unique Scientific Equipment in the Field of Nanotechnology (CCU MIPT) (Unique Identifier RFMEFI59417X0014). Part of the work was carried out using the equipment of the VNIIOFI Shared Facilities Centre for High-Precision Measurement Technologies in Photonics (http://www.ckp.vniiofi.ru/).

References

1. Sarychev A.K., Shalaev V.M. *Electrodynamics of Metamaterials* (World Scientific Publishing Co. Pte. Ltd., 2007).
2. Johnson P.B., Christy R.W. *Phys. Rev. B*, **6**, 4370 (1972).
3. Armani D.K., Kippenberg T.J., Spillane S.M., Vahala K.J. *Nature*, **421**, 925 (2003).
4. Herr T., Brasch V., Jost J.D., Mirgorodskiy I., Lihachev G., Gorodetsky M.L., Kippenberg T.J. *Phys. Rev. Lett*., **113**, 123901 (2014).
5. Savchenkov A.A., Matsko A.B., Ilchenko V.S., Maleki L. *Opt. Express*, **15**, 67 (2007).
6. Dumeige Y., Trebaol S., Ghisa L., Nguyen T.K., Tavernier H., Feron P. *J. Opt. Soc. Am. B*, **25**, 2073 (2008).
7. Gorodetsky M.L., Savchenkov A.A., Ilchenko V.S. *Opt. Lett*., **21**, 453 (1996).
8. Sumetsky M. *Opt. Lett*., **35**, 2385 (2010).
9. Dyknhe A.M., Sarychev A.K., Shalaev V.M. *Phys. Rev. B*, **67**, 195402 (2003).
10. Avrutsky I., Soref R., Buchwald W. *Opt. Express*, **18**, 348 (2010).
11. Avrutsky I., Salakhutdinov I., Elser J., Podolskiy V. *Phys. Rev. B*, **75**, 241402 (2007).
12. Sreekanth K.V., De Luca A., Strangi G. *Sci. Rep*., **3**, 3291 (2013).
13. Lagarkov A., Budashov I., Chistyaev V., Ezhov A., Fedyanin A., Ivanov A., Kurochkin I., Kosolobov S., Latyshev A., Nasimov D., Ryzhikov I., Shcherbakov M., Vaskin A., Sarychev A.K. *Opt. Express*, **24**, 7133 (2016).
14. Hong Y., Qiu Y., Chen T., Reinhard B.M. *Adv. Funct. Mater*., **24**, 739 (2014).
15. Hong Y., Pourmand M., Boriskina S.V., Reinhard B.M. *Adv. Mater*., **25**, 115 (2013).
16. Hong Y., Reinhard B.M. *Opt. Mater. Express*, **4**, 2409 (2014).
17. Pi S., Zeng X., Zhang N., Ji D., Chen B., Song H., Cheney A., Xu Y., Jiang S., Sun D., Song Y., Gan Q. *IEEE Photonics J*., **8**, 4800207 (2016).
18. Bryche J.-F., Gillibert R., Barbillon G., Gogol P., Moreau J., Lamy de la Chapelle M., Bartenlian B., Canva M. *Plasmonics*, **11**, 601 (2016).
19. Barbillon G., Sandana V.E., Humbert C., Belier B., Rogers D.J., Teherani F.H., Bove P., McClintock R., Razeghi M. *J. Mater. Chem. C*, **5**, 3528 (2017).
20. Sarychev A.K., Afanasev K.N., Bykov I.V., Boginskaya I.A., Ivanov A.V., Kurochkin I.N., Lagarkov A.N., Ryzhikov I.A., Sedova M.V., in *Proc. 2018 Int. Conf. Laser Optics (ICLO)* (IEEE, 2018) p. 558.
21. Sarychev A.K., Afanasev K.N., Bykov I.V., Boginskaya I.A., Evtushenko E.G., Ivanov A.V., Kurochkin I.N., Lagarkov A.N., Merzlikin A.M., Mikheev V.V., Negrov D.V., Ryzhikov I.A., Sedova M.V., in *Proc. 2018 Int. Conf. Laser Optics (ICLO)* (IEEE, 2018) p. 549.
22. Jahani S., Jacob Z. *Nat. Nanotechnol*., **11**, 23 (2016).
23. Roccapriore K.M., Lyvers D.P., Brown D.P., Poutrina E., Urbas A.M., Germer T.A., Drachev V.P. *Appl. Sci*., **8**, 617 (2018).
24. Lagarkov A., Boginkaya I., Bykov I., Budashov I., Ivanov A., Kurochkin I., Ryzhikov I., Rodionov I., Sedova M., Zverev A., Sarychev A.K. *Opt. Express*, **25**, 17021 (2017).
25. Sarychev A.K., Lagarkov A.N., Ivanov A.V., Boginskaya I.A., Bykov I.V., Ryzhikov I.A., Sedova M.V., Vaskin A.V., Kurochkin I.N., Rodionov I.A., Negrov D.V. *Proc. SPIE*, **10346**, 103460C1 (2017).
26. Afanasiev K.N., Boginskaya I.A., Budashov I.A., Ivanov A.V., Kurochkin I.S., Lagarkov A.N., Ryzhikov I.A., Sarychev A.K. *Proc. SPIE*, **9544**, 95441Y (2015).
27. Ivanov A.V., Boginskaya I.A., Vaskin A.V., Afanas'ev K.N., Ryzhikov I.A., Lagarkov A.N., Sarychev A., in *Proc. Int. Conf. 'Days on Diffraction 2015'* (IEEE, 2015) p. 146.
28. Ivanov A.V., Vaskin A.V., Lagarkov A.N., Sarychev A.K. *Proc. SPIE*, **9163**, 91633C (2014).
29. Kurochkin I.S., Ryzhikov I.A., Sarychev A.K., Afanasiev K.N., Budashov I.A., Sedova M.S., Boginskaya I.A., Amitonov S., Lagarkov A.N. *Adv. Electromagn*., **3** (1), 57 (2014).
30. Bandarenka H.V., Girel K.V., Bondarenko V.P., Khodasevich I.A., Panarin A.Y., Terekhov S.N. *Nanoscale Res. Lett*., **11**, 262 (2016).
31. Green M.A. *Solar Energy Materials & Solar Cells*, **92**, 1305 (2008).
32. Ignatov A.I., Merzlikin A.M., Baryshev A.V. *Phys. Rev. A*, **95**, 053843 (2017).
33. Maurel A., Felix S., Mercier J.-F., Ourir A., Djeffal Z.E. *J. Eur. Opt. Soc. Rap. Public*., **9**, 14001 (2014).
34. Christ A., Tikhodeev S.G., Gippius N.A., Kuhl J., Giessen H. *Phys. Rev. Lett*., **91**, 183901 (2003).
35. Campion A., Ivanecky J.E., Child C.M., Foster M. *J. Am. Chem. Soc*., **117**, 11807 (1995).
36. Kambhampati P., Child C.M., Foster M.C., Campion A. *J. Chem. Phys*., **108**, 5013 (1998).
37. Otto A. *J. Raman Spectrosc*., **36**, 497 (2005).